

Modeling Air Quality during the California Regional PM₁₀/PM_{2.5} Air Quality Study (CPRAQS) using the UCD/CIT Source Oriented Air Quality Model - Part III. Regional Source Apportionment of Secondary and Total Airborne PM_{2.5} and PM_{0.1}

Qi Ying^{a,b *}, Jin Lu^{a,b}, Ajith Kaduwela^b, and Michael J. Kleeman^{a †}

^aDepartment of Civil and Environmental Engineering
University of California, Davis. Davis, CA 95616

^bPlanning and Technical Support Division
California Air Resources Board, Sacramento CA, 95812

January 27, 2008

* Current address: Zachry Department of Civil and Environmental Engineering, Texas A&M University at College Station.

† Corresponding Author. Email: mjkleeman@ucdavis.edu

Abstract

A comprehensive air quality modeling project was carried out to simulate regional source contributions to secondary and total (=primary+secondary) airborne particle concentrations in California's central Valley. A three week stagnation episode lasting from December 15, 2000 to January 7, 2001, was chosen for study using the air quality and meteorological data collected during the California Regional PM₁₀/PM_{2.5} Air Quality Study (CRPAQS). The UCD/CIT mechanistic air quality model was used with explicit decomposition of the gas-phase reaction chemistry to track source contributions to secondary PM. Inert artificial tracers were used with an internal mixture representation to track source contributions to primary PM. Both primary and secondary source apportionment calculations were performed for 15 size fractions ranging from 0.01 - 10 μm particle diameter. Primary and secondary source contributions were resolved for fugitive dust, road dust, diesel engines, catalyst-equipped gasoline engines, non-catalyst-equipped gasoline engines, wood burning, food cooking, high sulfur fuel combustion, and other anthropogenic sources.

Diesel engines were identified as the largest source of secondary nitrate in central California during the study episode, accounting for approximately 40% of the total PM_{2.5} nitrate. Catalyst equipped gasoline engines were also significant, contributing approximately 20% of the total secondary PM_{2.5} nitrate. Agricultural sources were the dominant source of secondary ammonium ion. Sharp gradients of PM concentrations were predicted around major urban areas. The relative source contributions to PM_{2.5} from each source category in urban areas differ from those in rural areas, due to the dominance of primary OC in urban locations and secondary nitrate in the rural areas. The source contributions to ultra-fine particle mass PM_{0.1} also show clear urban/rural differences. Wood smoke was found to be the major source of PM_{0.1} in urban areas while motor vehicle sources were the major contributor of PM_{0.1} in rural areas, reflecting the influence from two major highways that transect the Valley.

1 Introduction

The San Joaquin Valley (SJV) experiences some of the worst wintertime particulate air quality pollution in the United States (American Lung Association, 2005). During the recent California Regional PM₁₀/PM_{2.5} Air Quality Study (CRPAQS), the fine PM concentration in the southern portion of the SJV reached a peak value of 200 $\mu\text{g m}^{-3}$ at Bakersfield (Chow et al., 2006). Approximately 50% of the PM_{2.5} was secondary ammonium nitrate that formed in the atmosphere from gas-phase precursors (Herner et al., 2005). The sources of this secondary PM can not be determined using traditional statistical source apportionment methods and so new techniques must be used to identify the origin of the winter PM problem in the SJV.

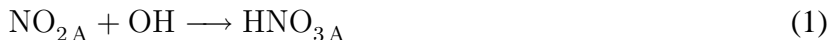
Mechanistic air quality models can predict changes in secondary PM concentrations in response to changes in precursor emissions (Stockwell et al., 2000; Pun and Seigneur, 2001). Mechanistic air quality models can also be used to identify source contributions to secondary PM (Mysliwiec and Kleeman, 2002; Kleeman et al., 2007). Previous modeling studies applied to a SJV winter air pollution episode that occurred in 1996 (Held et al., 2004) attempted to identify source contributions to the regional distribution of both the primary and secondary PM (Ying and Kleeman, 2006). This previous analysis was limited by the short duration of the study period (only three days) and the small size of the study domain (southern portion of the SJV only) leading to the conclusion that a large fraction of the secondary PM was transported from "upwind" sources or formed before the start of the three-day episode.

The wintertime CRPAQS study was designed to provide a larger spatial and temporal coverage of air quality and meteorology in the SJV to help better understand the sources and formation mechanisms of PM (Chow et al., 2006). The purpose of the current paper is to determine the regional source contributions to secondary PM during CRPAQS. Source contributions to total (=primary+secondary) PM_{2.5} and ultrafine PM (PM_{0.1}) are also discussed. This work, together with the base case simulation (Ying et al., 2008b) and regional primary source apportionment study (Ying et al., 2008a), represents the first source-oriented air quality model application to study the regional PM formation and source apportionment of PM over a multi-week episode during the

winter in central California.

2 Model Description

Regional source apportionment calculations for secondary PM are carried out using the source-oriented UCD/CIT air quality model. A comprehensive description of the UCD/CIT air quality model can be found in the base case paper (Ying et al., 2008b) and the references therein and so only the details related to source apportionment of secondary PM are discussed here. Source contributions to secondary PM are calculated with source-oriented gas phase chemistry and gas-to-particle partitioning (Mysliwiec and Kleeman, 2002). The source-oriented gas phase chemistry model tracks the precursor gases (NO_x , NH_3 and SO_2) emissions from different sources through the complex non-linear chemical reactions separately so that the source-origin of the semi-volatile products can be explicitly retained. For a simple example, NO_{2A} and NO_{2B} will be used to represent NO_2 from diesel engines and gasoline engines. The chain-termination reaction that produces the semi-volatile HNO_3 will be expanded into two reactions:



Writing separate equations for NO_{2A} and NO_{2B} allows us to separately quantify the buildup of HNO_{3A} and HNO_{3B} . In reality, a large number of chemical reactions and intermediate species need to be expanded to properly retain the source information for semi-volatile products such as nitrate, ammonium ion, and sulfate from multiple emission categories. This is accomplished using automated software that expands chemical reaction mechanisms written in the State Air Pollution Research Center (SAPRC) format. The gas-to-particle conversion routine that calculates the dynamic exchange of material between the gas and particle phases is also expanded to explicitly track semi-volatile products from each source category. Source-oriented concentrations for each semi-volatile species are aggregated during vapor pressure calculations so that the thermodynamics

package that calculates the surface vapor pressure of semi-volatile species is not modified. Concentrations of secondary organic aerosol are expected to be small during the cold winter conditions experienced during the current study, and so source apportionment of SOA is not considered in the current analysis.

The approach for the source apportionment of secondary PM described above is independent of the choice for primary particle representation in the model (internal mixture vs. source-oriented external mixture). When primary particles are tracked as a source-oriented external mixture, the secondary source apportionment calculations predict the amount of nitrate, sulfate, and ammonium ion originating for each source category that forms on primary particle cores released from each source category. As an example, it is possible that NO_x emitted from diesel engines can form nitrate on primary particles originally released from wood combustion. When primary particles are tracked as an internal mixture, the secondary source apportionment calculations still predict source contributions to secondary PM, but the source origin of the primary particle core is not known. The internal vs. external mixture representation for primary particles may influence the overall aerosol chemistry, especially during periods of high relative humidity (Kleeman et al., 1997). The sensitivity of total nitrate formation to internal vs. source-oriented external mixture treatments for primary particles will be discussed in the results section.

Several components of the UCD/CIT air quality model were updated in the current study in an attempt to improve the prediction of secondary nitrate formation during the wintertime episode. Recent experimental studies show that the accommodation coefficient (α) for N₂O₅ hydrolysis on wet particles is a function of particle composition (Riemer et al., 2003; Brown et al., 2006). The accommodation coefficient of N₂O₅ in the current model was revised from a constant value of 0.001 to be a function of aerosol sulfate and nitrate concentration, as shown in the equations 3 and 4 below, based on Riemer et al. (2003). The [S(VI)] and [N(V)] represent the particle sulfate and nitrate concentrations, respectively. This parameterization allows a higher accommodation coefficient for particles that are mainly sulfate and a lower coefficient for nitrate dominant particles. For particles that do not have any nitrate or sulfate, an accommodation coefficient of 0.002 is used.

$$f = \frac{[S(VI)]}{[S(VI)] + [N(V)]} \quad (3)$$

$$\alpha = 0.02 \times f + 0.002 \times (1.0 - f) \quad (4)$$

The gas phase pollutant dry deposition scheme used in the UCD/CIT air quality model was also updated in an attempt to improve nitrate predictions using the deposition model described by Walmsley and Wesely (1996). In the original UCD/CIT model, the dry deposition of SO₂ and O₃ is directly calculated based on a table of surface resistance as a function of the solar radiation intensity, and does not consider the possible change in the surface resistance due to seasonal variations (Russell et al., 1993). The deposition velocity of other species are either set as constant or scaled based on the SO₂ value. The Walmsley and Wesely scheme allows the direct determination of deposition velocities of 10 important gas species using the calculated solar intensity and the season-dependent surface resistance values. This modification allows the model to calculate dry deposition more accurately as a function of season and under different solar intensity conditions.

The sensitivity of predicted nitrate formation due to the changes described above will be discussed in section 5.

3 Model Application

The UCD/CIT source-oriented air quality model was configured to use internally mixed particle representation with artificial tracers for primary source apportionment and expanded reaction chemistry for secondary source apportionment. Model calculations were carried out for the period December 15, 2000 - January 7, 2001. Regional source contributions to secondary PM_{2.5}, total (=primary+secondary) PM_{2.5} and total PM_{0.1} were resolved for the entire central California region including the SJV. The source contributions to primary PM_{2.5} were calculated simultaneously with the secondary PM and the results are documented in a separate paper (Ying et al., 2008a). The

simulation was carried out using 4 km horizontal grid resolution with 190 x 190 grid cells in the domain that covers the entire central Valley of California. The computation domain covers land areas with surface elevation below 2000 meters and ocean regions up to 100 km from the coastline (see Figure 1 of Ying et al. (2008a)).

Details about the model configuration and the preparation of the model input fields describing meteorology, emissions, initial and boundary conditions are described by Ying et al. (2008b) and are not repeated here. Table 1 in Ying et al. (2008a) summarizes the domain-average emission totals of major pollutants and precursors. Gasoline engines and diesel engines are the two dominant sources of NO_x during the study episode. NO_x and VOC emissions from diesel engines are approximately twice as high as gasoline engines during the current study. This contrasts with the SJV emissions inventories for January 1996 (Held et al., 2004) where emissions from gasoline engines were estimated to be approximately twice as high as those from diesel engines. The implication of these emission trends for future emission control strategies will be discussed more comprehensively in a separate manuscript.

4 Results

The base case predictions of gas and particulate pollutant concentrations have been compared extensively with observations and shown to be satisfactory at most sites (Ying et al., 2008b). The UCD/CIT model predictions for source contributions to primary particulate matter were also found to be in good agreement with CMB predictions carried out using molecular markers (Ying et al., 2008a). These comparisons are necessary quality control checks on the model simulation that build confidence in the results of secondary source apportionment calculations can be considered.

UCD/CIT model calculations in the current study used an internal mixture particle representation with inert source tracers for primary source apportionment. Previous work has shown that the predicted source contributions to primary PM using the internal mixture approach are in good agreement with predictions made using a source-oriented external mixture particle representation

(Ying et al., 2008a). Figure 1 compares source contributions to secondary nitrate predictions made using internal vs. source-oriented external mixture particle representations. Different symbols on the figure correspond to different source categories. For each source category, the predicted concentrations at five stations (Bethel Island, Sacramento, Fresno, Angiola and Bakersfield) are shown on the figure. The source contributions predicted by the internally mixed model with artificial tracers agree closely with the source-oriented externally mixed aerosol approach. This is no surprise since both models use essentially the same expanded reaction chemistry for the source apportionment of secondary PM components. The regional difference in predicted total $PM_{2.5}$ nitrate concentration using the internal and external particle representation will be examined in section 5.4.

4.1 Source Apportionment of Secondary PM at Fresno

Figure 2 shows the predicted hourly-averaged relative source contributions to $PM_{2.5}$ nitrate (N(V)), sulfate (S(VI)), and ammonium ion (N(-III)) for Fresno during the study period. Panel 2(a) shows the calculated source contribution to $PM_{2.5}$ nitrate at Fresno. The initial concentration accounts for a major fraction of the nitrate in the beginning of the simulation but the initial conditions become negligible after two simulated days because most of these particles are advected out of the modeling domain. Previous studies have shown that dry deposition is not a significant fine particle removal mechanism compared to advection (Herner et al., 2006). Diesel engines are the main contributors to the secondary nitrate concentrations at Fresno, with an approximate relative contribution of 40%. Gasoline engines contribute about half as much nitrate as diesel engines. This differs from the previous SJV simulation (Ying and Kleeman, 2006) in which the contribution from gasoline engines was higher than the contribution from diesel engines. These changes reflect differences in the emissions inventory over time. Panel 2(b) shows that 80% of the predicted sulfate concentrations originated from background non-sea-salt sulfate. Local sulfate production is low due to the low emissions of SO_2 and slow SO_2 oxidation rates in cold winter conditions. Aqueous phase sulfate production was not considered in this simulation and is likely insignificant

due to low oxidants (O_3 and H_2O_2) concentrations. Panel 2(c) shows that approximately 80% of the ammonium ion originates from "other" sources that includes dairy operations. Approximately 10% of the ammonium ion originates from woodsmoke. Boundary conditions account for a further 10% of the ammonium ion, with slightly higher values during the day as the both the wind speed and mixing height increase. Contributions from catalyst equipped gasoline engines account for only a small fraction of the ammonium ion.

4.2 Regional Source Contribution to Secondary and Total PM

Figure 3(a) shows that predicted 24-hour average $PM_{2.5}$ nitrate concentrations on December 28, 2000 range from 10-20 $\mu g m^{-3}$ along the edges of the mountain boundaries to a maximum concentration of approximately 42 $\mu g m^{-3}$ in areas south east of Fresno. Contributions to $PM_{2.5}$ nitrate from wood smoke are not significant (Panel 3(b)). Panels 3(c), (d) and (e) show the contributions to $PM_{2.5}$ nitrate from diesel engines, non-catalyst equipped gasoline engines and catalyst equipped gasoline engines, respectively. Diesel engines and catalyst equipped gasoline engines are the two most important sources that contribute to the elevated secondary nitrate concentrations in the central Valley. The spatial distributions of nitrate from these three sources are similar, with high concentrations throughout most of the SJV. Predicted $PM_{2.5}$ nitrate concentrations are lower in the northern part of the central Valley due to significant wind ventilation that moves the pollutants to the San Francisco Bay area. The maximum $PM_{2.5}$ nitrate concentrations from diesel engines and catalyst equipped gasoline engines are approximately 19 and 11 $\mu g m^{-3}$, respectively. Non-catalyst gasoline engines have a maximum $PM_{2.5}$ nitrate contribution of 1.8 $\mu g m^{-3}$ and are not significant sources of particulate nitrate in the current study. Panel 3(f) shows that high sulfur fuel combustion makes a peak contribution of approximately 3 $\mu g m^{-3}$ to $PM_{2.5}$ nitrate in the area south east of Fresno. Panel 3(g) shows that other anthropogenic sources contribute less than 6 $\mu g m^{-3}$ of $PM_{2.5}$ nitrate in most portions of the Valley. At some isolated locations, the contribution from "other" sources can reach as high as 11 $\mu g m^{-3}$. Panel 3(h) shows a rather uniform $PM_{2.5}$ nitrate concentration of 4 $\mu g m^{-3}$ in the Valley from background NO_x sources.

Figure 4 shows the regional ammonium ion concentrations and the major sources that contribute to the predicted ammonium ion concentrations. Panel 4(a) shows that the predicted maximum 24-hour average $\text{PM}_{2.5}$ ammonium ion concentration on December 28, 2000 is approximately $15 \mu\text{g m}^{-3}$. Ammonium ion and nitrate have very similar spatial distributions since NH_3 tends to condense together with HNO_3 to neutralize the acidity of the particles. Panel 4(b) shows that the contribution of woodsmoke to ammonium ion is most noticeable in urban areas with a maximum 24-hour average contribution of $1.5 \mu\text{g m}^{-3}$. Contributions from non-catalyst equipped gasoline engines are small based on Panel 4(c). As shown in Panel 4(d), the ammonium ion concentration associated with catalyst-equipped gasoline engines reaches a maximum of $1.8 \mu\text{g m}^{-3}$ in the San Francisco Bay Area. Panel 4(e) shows that majority of the ammonium ion is from "other" sources that includes dairy emissions of NH_3 . The maximum "other" ammonium ion concentration coincides with the location of dairy operations in the central SJV between Fresno and Angiola. Panel 4(f) shows that the influence of background NH_3 is small, with approximately $0.5 \mu\text{g m}^{-3}$ of ammonium nitrate attributed to background sources near the computational boundary.

Figure 5 shows the major sources that contribute to the total (=primary+secondary) $\text{PM}_{2.5}$ mass concentrations on December 28, 2000. The dust category (5(a)) includes fugitive dust and paved road dust and is mainly composed of primary particles. Meat cooking(5(b)), and woodsmoke (5(c)) are also mainly composed of primary particles from urban centers. Woodsmoke dominates the total $\text{PM}_{2.5}$ mass concentrations with contributions as high as $60 \mu\text{g m}^{-3}$. The contributions from diesel engines (5(d)) includes primary elemental carbon (EC), primary organic compounds (OC), and secondary nitrate with a maximum total concentration of approximately $16 \mu\text{g m}^{-3}$. The primary contribution to the total diesel PM is higher in urban areas as most of the PM from diesel in rural areas of the central Valley is secondary (Figure 3). Non-catalyst equipped gasoline engines are not a major source of $\text{PM}_{2.5}$, reflecting their small contribution in the total vehicle fleet. The total $\text{PM}_{2.5}$ from catalyst equipped gasoline engines has a maximum concentration of $7.5 \mu\text{g m}^{-3}$. The results show that the contribution from catalyst equipped gasoline engines to total $\text{PM}_{2.5}$ is half that from diesel engines during the current study. This ratio reflects a change in

the diesel/gasoline emission ratio in the emission inventory since 1996 (Held et al., 2004). Diesel engines emit more NO_x but less VOC than gasoline engines, meaning that the ambient NO_x to VOC ratio in the SJV has also increased. The consequence of this emissions trend for summer ozone concentrations will require further investigation since the SJV currently violates the ozone National Ambient Air Quality Standards (NAAQS). High sulfur fuel combustion (5(h)) contributes significantly to $\text{PM}_{2.5}$ near the two air force bases in central California due to the use of high sulfur jet fuel. Approximately $30 \mu\text{g m}^{-3}$ of $\text{PM}_{2.5}$ in the SJV originates from sources that are not explicitly resolved in this study of which $15 \mu\text{g m}^{-3}$ is due to secondary ammonium ion (mainly from dairy sources) (Figure 4(f)) and $11 \mu\text{g m}^{-3}$ is secondary nitrate (Figure 3f). Panel 5(j) shows that background sources contribute approximately $9.5 \mu\text{g m}^{-3}$ of total $\text{PM}_{2.5}$ in the SJV. This material originates mainly from background NH_3 , NO_x and PAN that is gradually transformed into secondary PM during the study episode.

Figure 6 shows the calculated source contributions to total (=primary+secondary) $\text{PM}_{0.1}$ and $\text{PM}_{2.5}$ concentrations averaged over the entire modeling episode (December 15, 2000 - January 7, 2001) along a transect line in the Valley that passes through Bakersfield and Sacramento. The Lambert Y positions for Bakersfield and Sacramento are -177.3 and 174.9 km, respectively. Road dust and fugitive dust sources are combined into a single dust source category in this figure. Panel 6(a) shows the average source contribution to $\text{PM}_{0.1}$ mass. Two sharp concentration peaks can be seen around Bakersfield and Sacramento. The concentration gradient is most significant around Bakersfield, where concentrations decrease by a factor of 10 in approximately 25 km. $\text{PM}_{0.1}$ concentrations between the two major urban areas are much lower (approximately $2.5 \mu\text{g m}^{-3}$) and relatively uniform. Wood smoke accounts for a majority of the ultra-fine particle mass ($\text{PM}_{0.1}$) in the urban areas while particles from transportation related sources account for larger fractions of $\text{PM}_{0.1}$ in rural areas. Model calculations predict that most of the $\text{PM}_{0.1}$ mass is composed of primary EC and OC.

Panel 6(b) shows the source contributions to total (=primary+secondary) $\text{PM}_{2.5}$ mass concentrations along the Bakersfield-Sacramento transect line averaged over the entire study period. The

maximum concentrations occur in area surrounding Bakersfield, with the highest predicted concentration approaching $80 \mu\text{g m}^{-3}$. The urban peak of Sacramento can also be seen on the figure with highest episode-average concentration reaching approximately $55 \mu\text{g m}^{-3}$. The largest sources of $\text{PM}_{2.5}$ concentrations in these two urban areas are wood smoke and diesel engines. The $\text{PM}_{2.5}$ concentrations in the rural areas are also high, with maximum episode-average concentrations of $60 \mu\text{g m}^{-3}$ in areas between Fresno and Angiola. Secondary ammonium nitrate dominates the $\text{PM}_{2.5}$ concentrations in the rural area, with most of the nitrate originating from diesel and gasoline engines. A significant contribution from the "other" source includes ammonium ion from animal sources. The contribution of dust particles to the average $\text{PM}_{2.5}$ concentrations are likely over-estimated (see section 4.1). The episode-average (24-day) $\text{PM}_{2.5}$ concentrations along this transect line in the Valley are higher than the newly proposed 24-hour average $\text{PM}_{2.5}$ NAAQS of $35 \mu\text{g m}^{-3}$.

Diesel engines are the largest source of secondary nitrate in central California during the study episode (40%), followed by catalyst equipped gasoline engines (20%). The relative source contributions to $\text{PM}_{2.5}$ from each source category in urban areas differ from those in rural areas, due to the dominance of secondary nitrate in the total $\text{PM}_{2.5}$ mass concentration in the rural areas. The predicted source contributions to ultra-fine particles also show clear urban/rural differences. Wood smoke is the major source of $\text{PM}_{0.1}$ in urban areas while motor vehicle sources are the major contributor of $\text{PM}_{0.1}$ in rural areas, reflecting the influence from two major highways that transect the Valley.

5 Sensitivity Analysis for Nitrate Formation

Previous work has shown that the UCD/CIT model captures regional nitrate formation mechanisms adequately but under-predicts local nitrate formation at Bakersfield during the latter portion of the current study. The impact of several parameters that affect nitrate formation were studied to identify the importance of each parameter in an attempt to explain the nitrate under-prediction at

5.1 Dry Deposition

The original dry deposition scheme used by the UCD/CIT air quality model was developed for a summer smog simulation in Southern California (Russell et al., 1993) and so the estimated deposition rates are higher than the deposition rates calculated by the Walmsley and Wesely scheme for the winter season. It is expected that enhanced HNO_3 deposition predicted by the original scheme will lead to lower nitrate concentrations. A sensitivity run using the original dry deposition scheme was used to quantify this effect. Figure 7 (a) shows that the Walmsley and Wesely scheme leads to an increase of approximately $6 \mu\text{g m}^{-3}$ in the predicted 24-hour averaged nitrate concentrations on December 28, 2000, due to lower dry deposition velocities.

5.2 Temperature Variation

Temperature is also a key factor that affects the nitrate formation. Gas/particle equilibrium of ammonium nitrate is highly temperature dependent (Aw and Kleeman, 2003). Increased temperature moves the gas/particle equilibrium toward gas phase. Another competing effect is that the chemical reaction rates are also temperature dependent. Higher temperature leads to higher reaction rates and increased production of nitric acid. The input temperature for model calculations was uniformly decreased by 2°C to study the effect on nitrate formation during the current study. The relative humidity was held constant during this simulation. Figure 7(b) shows that lowering the temperature by two degrees uniformly decreased 24-hour averaged nitrate concentrations in the central Valley on December 28, 2000, by approximately $1\text{-}2 \mu\text{g m}^{-3}$. The results indicate that temperature effects on reaction rates are more significant than temperature effects on gas/particle partitioning under the current meteorological conditions.

5.3 N₂O₅ Accommodation Coefficient

The N₂O₅ accommodation coefficient describes the probability that a N₂O₅ molecule that strikes a particle surface will stick. The heterogeneous reaction of N₂O₅ on particle surfaces is one of the most important pathways for the formation of secondary nitrate (Jacob, 2000). Accommodation coefficients used in previous modeling studies have varied significantly from 0.005 to 0.1 and may also be particle composition dependent (Evans and Jacob, 2005). An additional simulation was performed in the current study using a fixed N₂O₅ accommodation coefficient of 0.001 to test the upper limit of N₂O₅ hydrolysis during winter conditions in central California. Figure 7(c) shows the change of 24-hour average nitrate concentrations on December 28, 2000 when this change was made. Nitrate concentrations decreased by approximately $2 \mu\text{g m}^{-3}$ in the northern portion of the Valley due to a lower N₂O₅ accommodation coefficient. In the southern part of the Valley, nitrate concentrations decreased by as much as $8 \mu\text{g m}^{-3}$ in the region south of Bakersfield. These results indicate that N₂O₅ heterogeneous reaction is a significant pathway of wintertime particulate nitrate formation in the SJV and the amount of nitrate formed is quite sensitive to the selection of N₂O₅ accommodation coefficient.

5.4 Internal/External Particle Representation

The internal mixture particle representation was used to generate the results presented in the previous sections. The source-oriented externally mixed particle representation is a more accurate way of representing particles in urban and regional airborne particles. Figure 7(d) shows the change of the predicted 24-hour average nitrate concentrations on December 28, 2000 using the source-oriented externally and internally mixed particle representations. Under the current modeling episode, little difference in the predicted nitrate concentration is noticed using the two different particle representations. The close agreement of the internally mixed and externally mixed results ensures that the internally mixed particle representation can be used as a base case calculation and future modeling studies.

6 Conclusions

Diesel engines are the largest source of secondary nitrate in central California during the study episode, accounting for approximately 40% of the total $PM_{2.5}$ nitrate. Catalyst equipped gasoline engines are also significant sources of secondary nitrate, contributing approximately 20% of the $PM_{2.5}$ nitrate. Sharp gradients of total (=primary+secondary) PM concentrations were predicted around major urban areas. The relative source contributions to total $PM_{2.5}$ from each source category in urban areas differ from those in rural areas, due to the dominance of primary OC in urban locations and secondary nitrate in the rural areas. The source contributions to ultra-fine particles also show clear urban/rural differences. Wood smoke is the major source of $PM_{0.1}$ in urban areas while motor vehicle sources are the major contributor of $PM_{0.1}$ in rural areas, reflecting the influence from two major highways that transect the Valley.

Acknowledgment

This research is supported by the California Air Resources Board. The statements, opinions, findings, and conclusions of this paper are those of the authors and do not necessarily represent the views of the California Air Resources Board. The authors thank Dr. John Watson and Dr. Douglas Lowenthal at the Desert Research Institute for CMB source apportionment results.

References

- American Lung Association. State of the air 2005. Technical report, 2005.
- J. Aw and M. J. Kleeman. Evaluating the first-order effect of intraannual temperature variability on urban air pollution. *Journal of Geophysical Research-Atmospheres*, 108(D12), 2003.
- S. S. Brown, T. B. Ryerson, A. G. Wollny, C. A. Brock, R. Peltier, A. P. Sullivan, R. J. Weber, W. P. Dube, M. Trainer, J. F. Meagher, F. C. Fehsenfeld, and A. R. Ravishankara. Variability in nocturnal nitrogen oxide processing and its role in regional air quality. *Science*, 331:67–70, 2006.
- J. C. Chow, L. W. A. Chen, J. G. Watson, D. H. Lowenthal, K. A. Magliano, K. Turkiewicz, and D. E. Lehrman. PM_{2.5} chemical composition and spatiotemporal variability during the California regional PM₁₀/PM_{2.5} air quality study (CRPAQS). *Journal of Geophysical Research-Atmospheres*, 111(D10), 2006.
- M. J. Evans and D. J. Jacob. Impact of new laboratory studies of n₂o₅ hydrolysis on global model budgets of tropospheric nitrogen oxides, ozone, and oh. *GEOPHYSICAL RESEARCH LETTERS*, 32(L09813), 2005.
- T. Held, Q. Ying, A. Kaduwela, and M. Kleeman. Modeling particulate matter in the San Joaquin Valley with a source-oriented externally mixed three-dimensional photochemical grid model. *Atmospheric Environment*, 38(22):3689–3711, 2004.
- J. Herner, Q. Ying, J. Aw, O. Gao, D. Chang, and M. Kleeman. Dominant mechanisms that shape the airborne particle size and composition distribution in central california. *Aerosol Science and Technology*, 2006.
- J. D. Herner, J. Aw, O. Gao, D. P. Chang, and M. J. Kleeman. Size and composition distribution of airborne particulate matter in northern California: I-particulate mass, carbon, and water-soluble ions. *Journal of the Air & Waste Management Association*, 55(1):30–51, 2005.
- D. J. Jacob. Heterogeneous chemistry and tropospheric ozone. *Atmospheric Environment*, 34(12): 2131–2159, 2000.
- M. J. Kleeman, G. R. Cass, and A. Eldering. Modeling the airborne particle complex as a source-oriented external mixture. *Journal of Geophysical Research-Atmospheres*, 102(D17):21355–21372, 1997.
- M. J. Kleeman, Q. Ying, J. Lu, M. J. Mysliwicz, R. J. Griffin, J. J. Chen, and S. Clegg. Source apportionment of secondary organic aerosol during a severe photochemical smog episode. *Atmospheric Environment*, 41(3):576–591, 2007.
- M. J. Mysliwicz and M. J. Kleeman. Source apportionment of secondary airborne particulate matter in a polluted atmosphere. *Environmental Science & Technology*, 36(24):5376–5384, 2002.

- B. K. Pun and C. Seigneur. Sensitivity of particulate matter nitrate formation to precursor emissions in the California San Joaquin Valley. *Environmental Science & Technology*, 35(14):2979–2987, 2001.
- N. Riemer, H. Vogel, B. Vogel, B. Schell, I. Ackermann, C. Kessler, and H. Hass. Impact of the heterogeneous hydrolysis of N_2O_5 on chemistry and nitrate aerosol formation in the lower troposphere under photosmog conditions. *Journal of Geophysical Research-Atmospheres*, 108 (D4), 2003.
- A. G. Russell, D. A. Winner, R. A. Harley, K. F. McCue, and G. R. Cass. Mathematical-modeling and control of the dry deposition flux of nitrogen-containing air-pollutants. *Environmental Science & Technology*, 27(13):2772–2782, 1993.
- W. R. Stockwell, J. G. Watson, N. F. Robinson, W. Steiner, and W. W. Sylte. The ammonium nitrate particle equivalent of nox emissions for wintertime conditions in central California’s San Joaquin Valley. *Atmospheric Environment*, 34(27):4711–4717, 2000.
- J. L. Walmsley and M. L. Wesely. Modification of coded parametrizations of surface resistances to gaseous dry deposition. *Atmospheric Environment*, 30(7):1181–1188, 1996.
- Q. Ying and M. J. Kleeman. Source contributions to the regional distribution of secondary particulate matter in California. *Atmospheric Environment*, 40(4):736–752, 2006.
- Q. Ying, J. Lu, and M. J. Kleeman. Modeling air quality during the California Regional PM10/PM2.5 Air Quality Study (CRPAQS) using the CIT/UCD source oriented air quality model - Part II. source apportionment of primary particulate matter. *Atmospheric Environment*, Submitted, 2008a.
- Q. Ying, J. Lu, P. Livingstone, P. Allen, and M. J. Kleeman. Modeling air quality during the California Regional PM10/PM2.5 Air Quality Study (CRPAQS) using the CIT/UCD source oriented air quality model - Part I. Base case model results. *Atmospheric Environment*, Submitted, 2008b.

List of Figures

1	Source contribution to the 24-hour average $PM_{2.5}$ nitrate on December 26, 2000 calculated using the externally mixed aerosol model and the internal mixture with artificial tracer model. Different symbols represent different emission source categories. The data points included in the figures are predicted concentrations at Bethel Island, Sacramento, Fresno, Angiola and Bakersfield	19
2	Relative source contribution to $PM_{2.5}$ nitrate, sulfate, ammonium ion and PM mass at Fresno from December 15, 2000 to January 7, 2001	20
3	Source contribution to $PM_{2.5}$ nitrate concentrations on December 28, 2000 The scale on each panel is different. Units are $\mu g m^{-3}$	21
4	Source contribution to $PM_{2.5}$ ammonium ion concentrations on December 28, 2000 The scale on each panel is different. Units are $\mu g m^{-3}$	22
5	Source contribution to total $PM_{2.5}$ mass concentrations on December 28, 2000 The scale on each panel is different. Units are $\mu g m^{-3}$	23
6	Source contribution to $PM_{0.1}$ and $PM_{2.5}$ along a line passing through Sacramento and Bakersfield averaged from December 15, 2000 to January 7, 2001	24
7	Change in 24-hour average $PM_{2.5}$ nitrate concentrations on December 28, 2000 due to (a) updated deposition scheme, (b) -2 °C temperature change, (c) lower N_2O_5 accommodation coefficient and (d) external vs. internal particle representation. Units are in $\mu g m^{-3}$	25

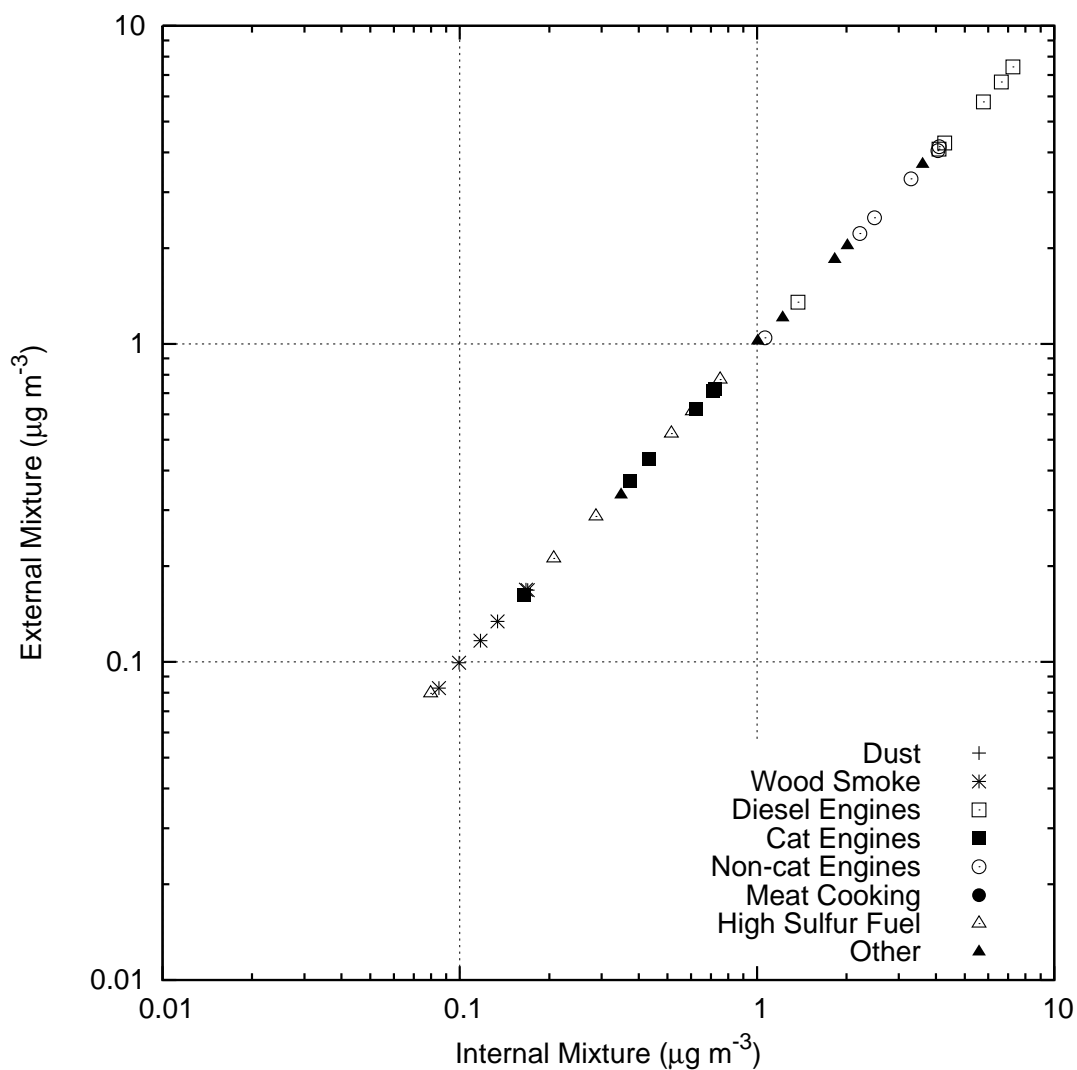
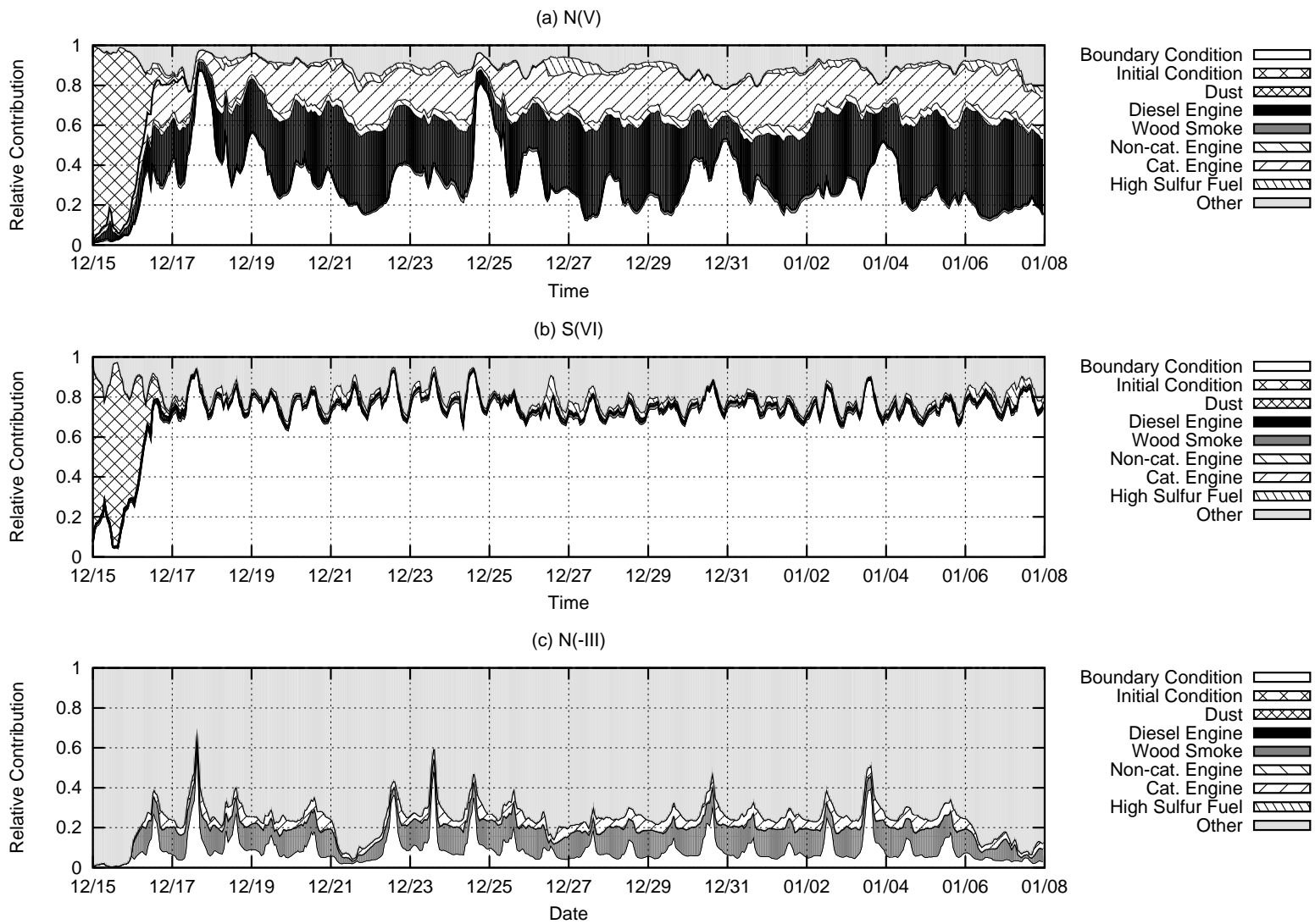


Figure 1: Source contribution to the 24-hour average $\text{PM}_{2.5}$ nitrate on December 26, 2000 calculated using the externally mixed aerosol model and the internal mixture with artificial tracer model. Different symbols represent different emission source categories. The data points included in the figures are predicted concentrations at Bethel Island, Sacramento, Fresno, Angiola and Bakersfield

Figure 2: Relative source contribution to $PM_{2.5}$ nitrate, sulfate, ammonium ion and PM mass at Fresno from December 15, 2000 to January 7, 2001



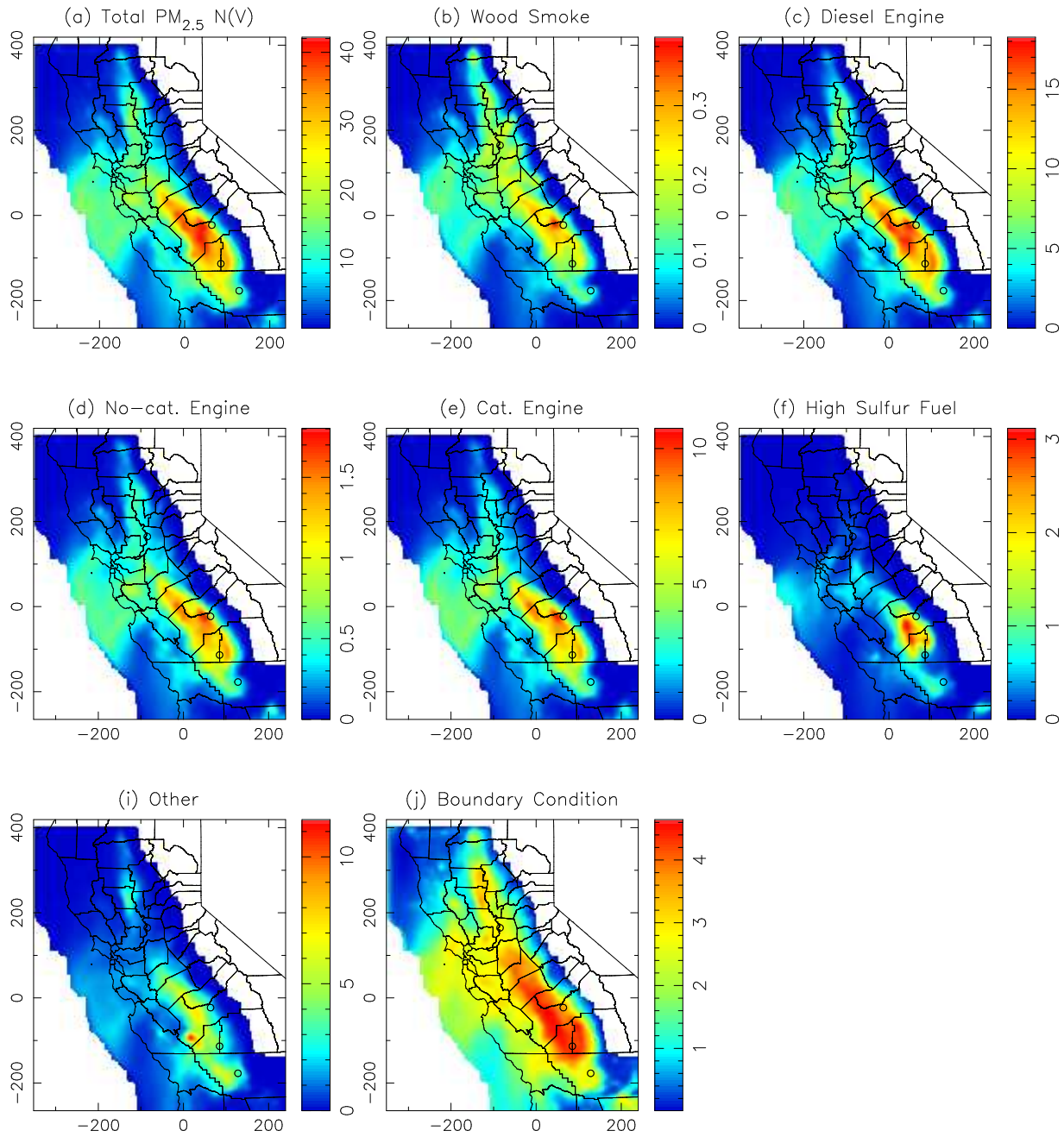


Figure 3: Source contribution to $\text{PM}_{2.5}$ nitrate concentrations on December 28, 2000 The scale on each panel is different. Units are $\mu\text{g m}^{-3}$

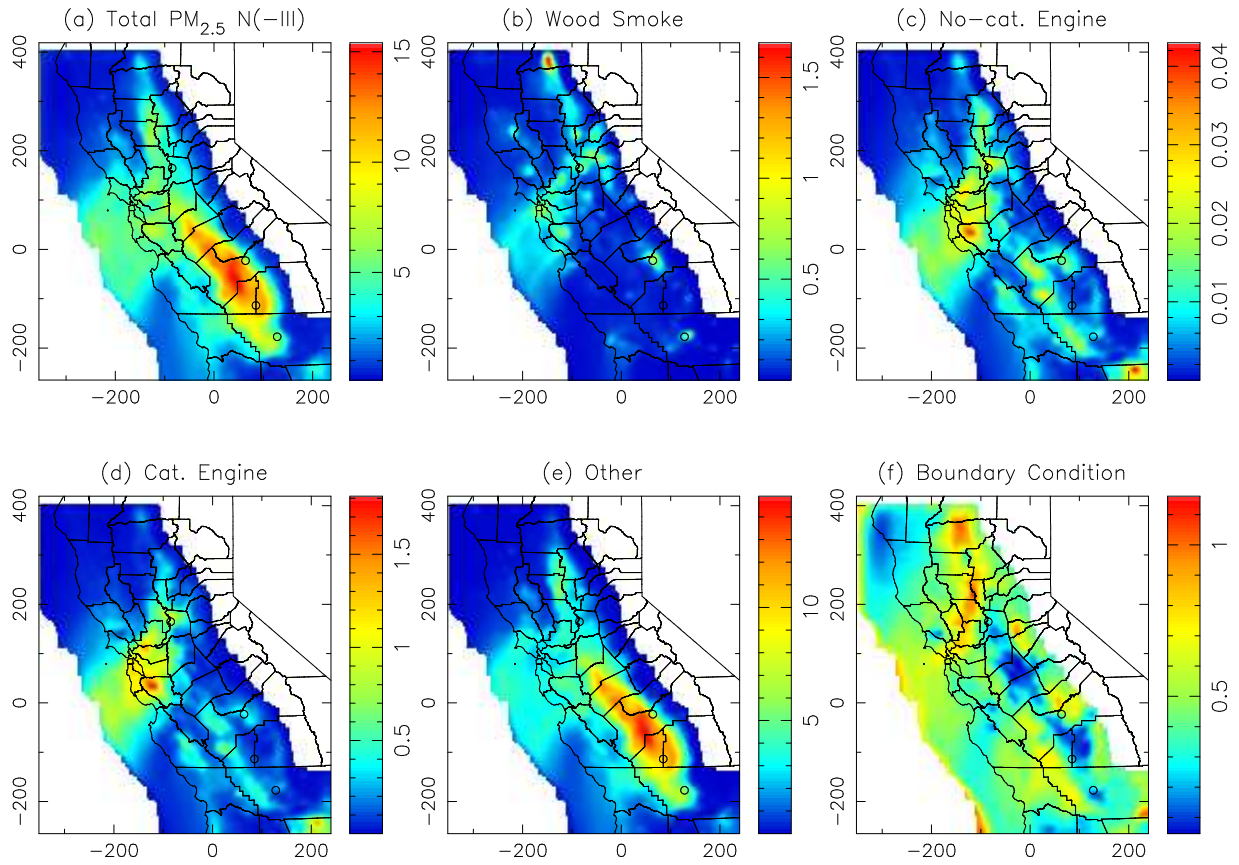


Figure 4: Source contribution to $PM_{2.5}$ ammonium ion concentrations on December 28, 2000. The scale on each panel is different. Units are $\mu g m^{-3}$.

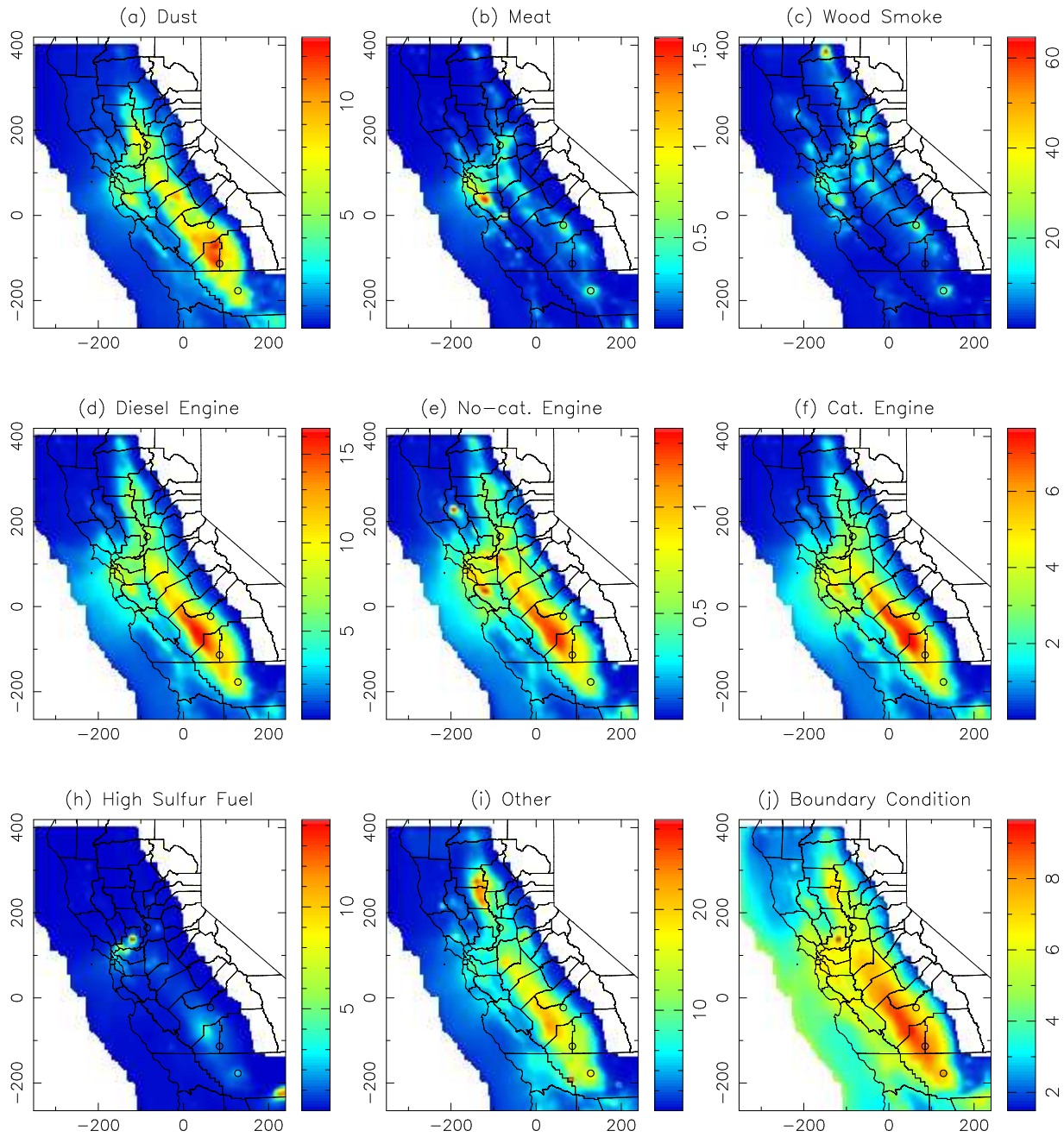


Figure 5: Source contribution to total $PM_{2.5}$ mass concentrations on December 28, 2000. The scale on each panel is different. Units are $\mu g m^{-3}$.

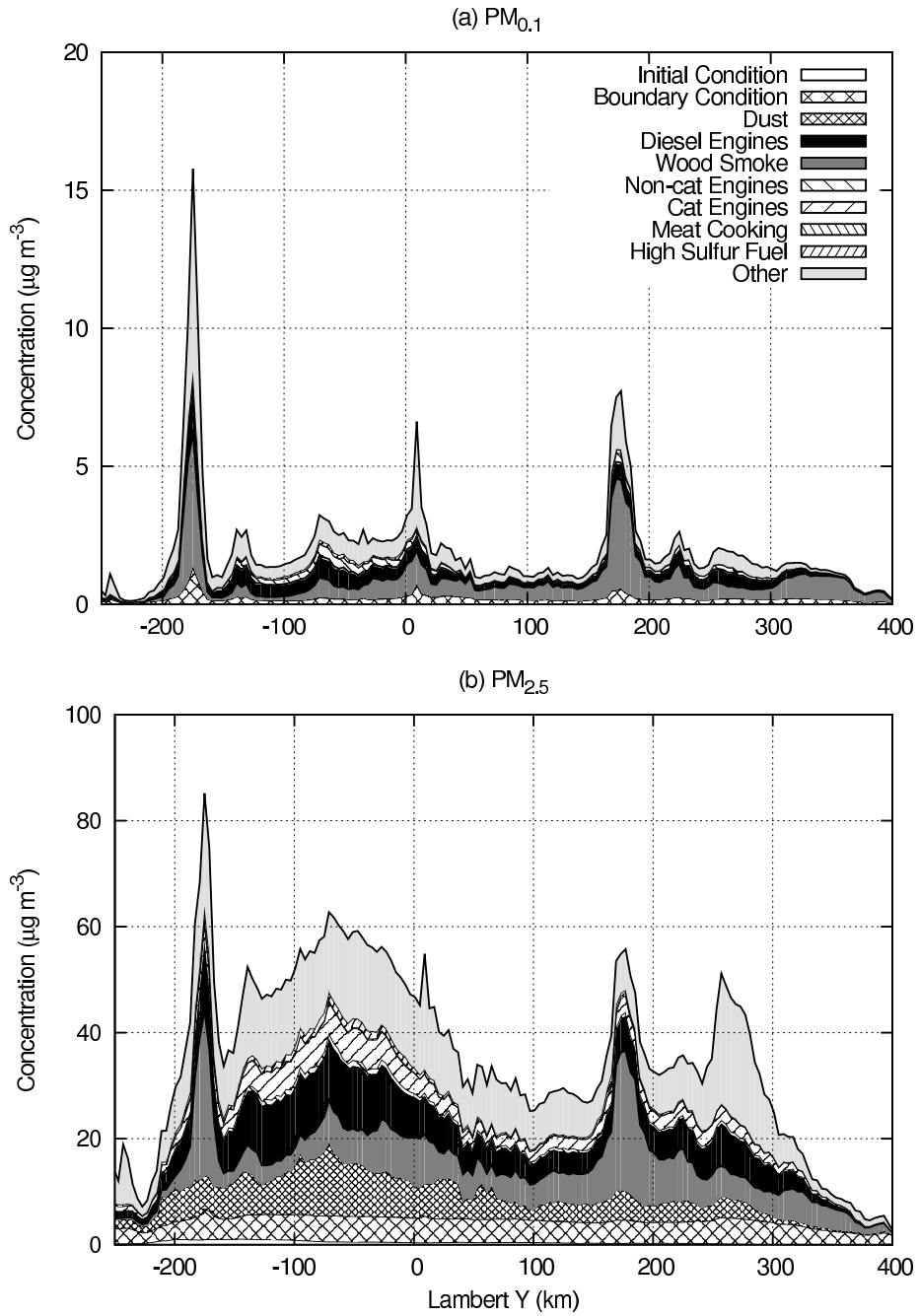


Figure 6: Source contribution to $PM_{0.1}$ and $PM_{2.5}$ along a line passing through Sacramento and Bakersfield averaged from December 15, 2000 to January 7, 2001

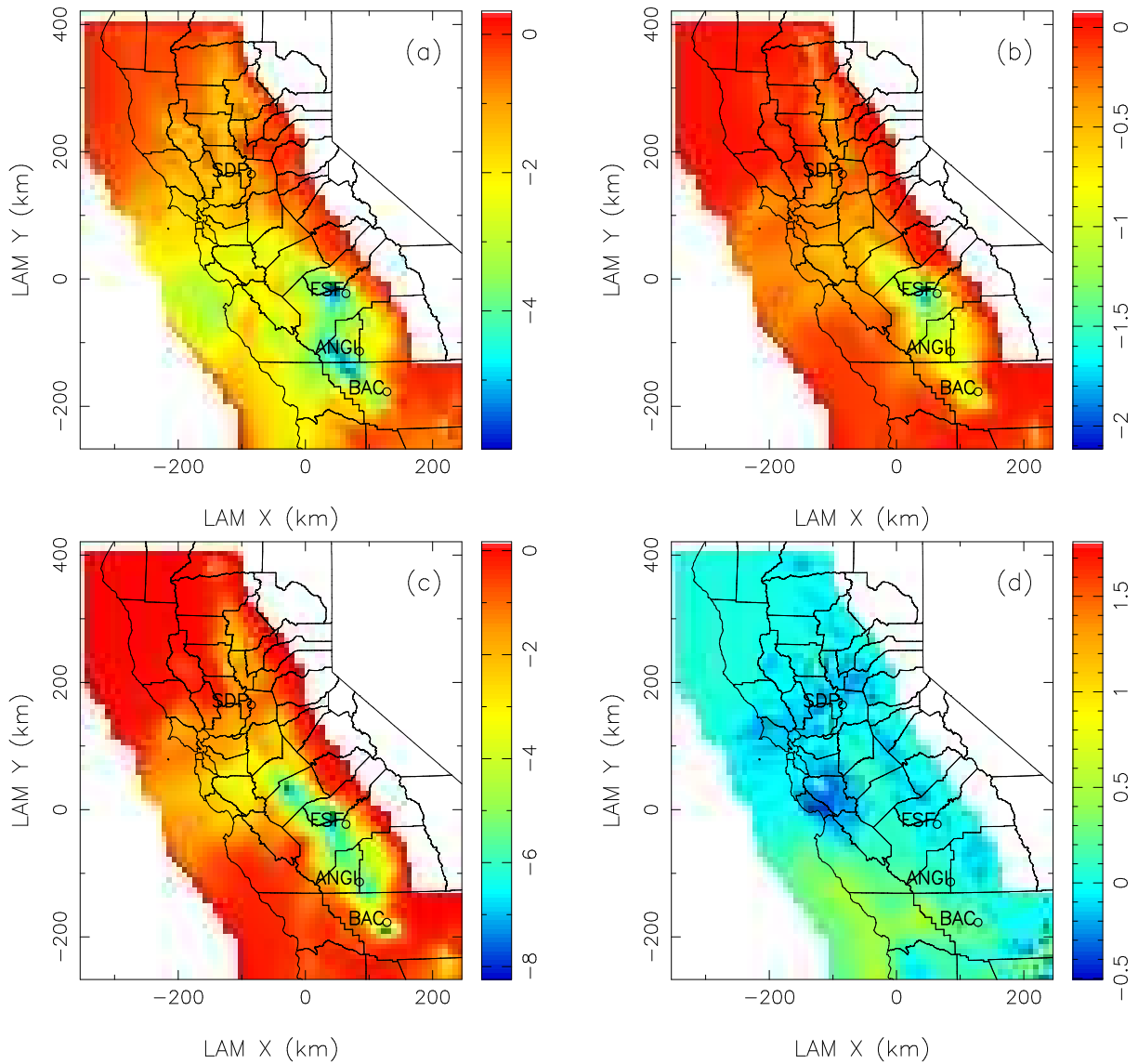


Figure 7: Change in 24-hour average PM_{2.5} nitrate concentrations on December 28, 2000 due to (a) updated deposition scheme, (b) -2 °C temperature change, (c) lower N₂O₅ accommodation coefficient and (d) external vs. internal particle representation. Units are in $\mu\text{g m}^{-3}$